A Section 508–conformant HTML version of this article is available at https://doi.org/10.1289/EHP5139.

Acute Methylmercury Exposure and the Hypoxia-Inducible Factor-1α Signaling Pathway under Normoxic Conditions in the Rat Brain and Astrocytes *in Vitro*

Jie Chang,[1] Bobo Yang,[1*] Yun Zhou,[1*] Changsheng Yin,[2,1] Tingting Liu,[1] Hai Qian,[1] Guangwei Xing,[1] Suhua Wang,[1] Fang Li,[1] Yubin Zhang,[3] Da Chen,[4] Michael Aschner,[5] and Rongzhu Lu[1,6]*

[1]Department of Preventive Medicine and Public Health Laboratory Sciences, School of Medicine, Jiangsu University, Zhenjiang, China
[2]Institute of Life Sciences, Jiangsu University, Zhenjiang, China
[3]Department of Occupational Health and Toxicology, School of Public Health, Fudan University, Shanghai, China
[4]School of Environment, Guangdong Key Laboratory of Environmental Pollution and Health, Jinan University, Guangzhou, China
[5]Department of Molecular Pharmacology, Albert Einstein College of Medicine, Bronx, New York, USA
[6]Center for Experimental Research, Kunshan Hospital Affiliated to Jiangsu University, Kunshan, China

Background: As a ubiquitous environmental pollutant, methylmercury (MeHg) induces toxic effects in the nervous system, one of its main targets. However, the exact mechanisms of its neurotoxicity have not been fully elucidated. Hypoxia-inducible factor-1α (HIF-1α), a transcription factor, plays a crucial role in adaptive and cytoprotective responses in cells and is involved in cell survival, proliferation, apoptosis, inflammation, angiogenesis, glucose metabolism, erythropoiesis, and other physiological activities.

Objectives: The aim of this study was to explore the role of HIF-1α in response to acute MeHg exposure in rat brain and primary cultured astrocytes to improve understanding of the mechanisms of MeHg-induced neurotoxicity and the development of effective neuroprotective strategies.

Methods: Primary rat astrocytes were treated with MeHg (0–10 μM) for 0.5 h. Cell proliferation and cytotoxicity were assessed with a 3-(4,5-dimethylthiazol-2-yl)-2,5-diphenyl diphenyltetrazolium bromide (MTT) assay and a lactate dehydrogenase (LDH) release assay, respectively. Reactive oxygen species (ROS) levels were analyzed to assess the level of oxidative stress using 2′,7′-dichlorofluorescin diacetate (DCFH-DA) fluorescence. HIF-1α, and its downstream proteins, glucose transporter 1 (GLUT-1), erythropoietin (EPO), and vascular endothelial growth factor A (VEGF-A) were analyzed by means of Western blotting. Real-time PCR was used to detect the expression of HIF-1α mRNA. Pretreatment with protein synthesis inhibitor (CHX), proteasome inhibitor (MG132), or proline hydroxylase inhibitor (DHB) were applied to explore the possible mechanisms of HIF-1α inhibition by MeHg. To investigate the role of HIF-1α in MeHg-induced neurotoxicity, cobalt chloride ($CoCl_2$), 2-methoxyestradiol (2-MeOE2), small interfering RNA (siRNA) transfection and adenovirus overexpression were used. Pretreatment with *N*-acetyl-L-cysteine (NAC) and vitamin E (Trolox) were used to investigate the putative role of oxidative stress in MeHg-induced alterations in HIF-1α levels. The expression of HIF-1α and related downstream proteins was detected in adult rat brain exposed to MeHg (0–10 mg/kg) for 0.5 h *in vivo*.

Results: MeHg caused lower cell proliferation and higher cytotoxicity in primary rat astrocytes in a time- and concentration-dependent manner. In comparison with the control cells, exposure to 10 μM MeHg for 0.5 h significantly inhibited the expression of astrocytic HIF-1α, and the downstream genes GLUT-1, EPO, and VEGF-A ($p < 0.05$), in the absence of a significant decrease in HIF-1α mRNA levels. When protein synthesis was inhibited by CHX, MeHg promoted the degradation rate of HIF-1α. MG132 and DHB significantly blocked the MeHg-induced decrease in HIF-1α expression ($p < 0.05$). Overexpression of HIF-1α significantly attenuated the decline in MeHg-induced cell proliferation, whereas the inhibition of HIF-1α significantly increased the decline in cell proliferation ($p < 0.05$). NAC and Trolox, two established antioxidants, reversed the MeHg-induced decline in HIF-1α protein levels and the decrease in cell proliferation ($p < 0.05$). MeHg suppressed the expression of HIF-1α and related downstream target proteins in adult rat brain.

Discussion: MeHg induced a significant reduction in HIF-1α protein by activating proline hydroxylase (PHD) and the ubiquitin proteasome system (UPS) in primary rat astrocytes. Additionally, ROS scavenging by antioxidants played a neuroprotective role via increasing HIF-1α expression in response to MeHg toxicity. Moreover, we established that up-regulation of HIF-1α might serve to mitigate the acute toxicity of MeHg in astrocytes, affording a novel therapeutic target for future exploration. https://doi.org/10.1289/EHP5139

Introduction

Methylmercury (MeHg) is a global environmental contaminant targeting the central nervous system (CNS) (Farina and Aschner 2017; Santos et al. 2016). Consumption of MeHg-containing fish products (Canuel et al. 2006; Carrasco et al. 2011; Steuerwald et al. 2000; Stopford and Goldwater 1975) and rice (Rothenberg et al. 2014; Zhang et al. 2010) has been shown to induce neurodegeneration as well as be associated with neurodevelopmental disorders (Belletti et al. 2002; Carocci et al. 2014; Ceccatelli et al. 2010). However, the underlying cellular and molecular mechanisms of MeHg-induced neurotoxicity have yet to be fully elucidated. Meanwhile, there is still a lack of treatment to effectively protect against MeHg-induced brain damage.

Hypoxia-inducible factor-1 (HIF-1), a DNA-binding transcription factor, plays a crucial role in a diverse range of adaptive responses to oxygen tension. HIF-1 is a heterodimer comprising an oxygen-labile α-submit (HIF-1α) and a constitutively expressed β-submit (HIF-1β). Under normal oxygen conditions (>5% O_2), prolyl hydroxylase (PHD) has been shown to mediate hydroxylation of HIF-1α (Berra et al. 2003; Ivan et al. 2001). Hydroxylated HIF-1α is rapidly degraded by the ubiquitin proteasome system (UPS), mediated by interaction with the von-Hippel Lindau tumor suppressor gene product (pVHL) (Bruick and McKnight, 2001; Lee et al. 2007). Under hypoxic conditions (<5% O_2) or stimulation by other environmental factors, stabilized HIF-1α dimerizes with HIF-1β to transactivate a series of adaptive genes, including vascular endothelial growth factor A (VEGF-A), glucose transporter 1 (GLUT-1), and erythropoietin (EPO) (Semenza and Wang, 1992). Several metals and organic chemicals have been shown to affect HIF-1α expression and activity (Dong et al. 2016; Lee et al. 2009; Liao et al. 2014; Wikenheiser et al. 2013; Wu et al.

*These authors contributed equally to this work as first authors.

Address correspondence to Dr. Rongzhu Lu, Department of Preventive Medicine and Public Health Laboratory Sciences, School of Medicine, Jiangsu University, 301 Xuefu Road, Zhenjiang, Jiangsu 212013. Telephone: +86 511 85038449; Fax: +86 511 85038483. Email: Lurz@ujs.edu.cn

The authors declare they have no actual or potential competing financial interests.

Received 10 February 2019; Revised 7 November 2019; Accepted 18 November 2019; Published 18 December 2019.

Note to readers with disabilities: *EHP* strives to ensure that all journal content is accessible to all readers. However, some figures and Supplemental Material published in *EHP* articles may not conform to 508 standards due to the complexity of the information being presented. If you need assistance accessing journal content, please contact ehponline@niehs.nih.gov. Our staff will work with you to assess and meet your accessibility needs within 3 working days.

2010), whereas increased expression of HIF-1α has been shown to be protective against neurotoxicants (Feng et al. 2014; Lee et al. 2009; Wu et al. 2010). Manganese has also been shown to increase HIF-1α protein levels in Hep2 cells by regulating mitogen-activated protein kinases (MAPKs) (Shin et al. 2010). Clioquinol (a copper and zinc chelator) decreased HIF-1α degradation by inhibiting HIF-1α ubiquitination and hydroxylation in SH-SY5Y cells and HepG2 cells, whereas addition of copper and zinc reversed these effects (Choi et al. 2006). Cadmium was shown to up-regulate HIF-1α expression in human lung epithelial cells via the production of reactive oxygen species (ROS) through the activation of the protein kinase B (Akt), and extracellular signal-regulated protein kinase (ERK) signaling pathways (Jing et al. 2012). Notably, deferoxamine (DFO), an iron chelator, was shown to attenuate neuronal cell death and the generation of ROS caused by MeHg and methylphenyl tetrahydropyridine (MPTP) in *in vivo* rodent models (Guo et al. 2016; LeBel et al. 1992). Furthermore, it was shown that by inhibiting the activity of proline hydroxylase (PHD) in mouse hippocampal neurons, DFO decreased degradation of HIF-1α and increased intracellular levels of HIF-1α protein (Hamrick et al. 2005). Recently, several studies have further documented that HIF-1α is neuroprotective because it drives the expression of critical genes that diminish neuronal cell death (Chen et al. 2017; Sen and Sen 2016). Increased HIF-1α expression and activity have been shown to promote glycolysis and glucose metabolism, thus countering oxidative stress by producing NADH and NADPH to propagate neuroprotective responses (Soucek et al. 2003). HIF-1α has also been shown to improve cerebral blood flow, which could oppose the toxicity of hypoxia (Iyalomhe et al. 2017). Overexpression of HIF-1α and/or HIF-1α target genes, such as VEGF-A and EPO, may be an early adaptation to the oxidative stressors that characterize MeHg-induced neuropathology. Thus, we speculate that the molecular events that constitute this early adaptation are likely neuroprotective and might mitigate neuronal injury caused by MeHg.

Previous studies have indicated an association between HIF-1α activity and intracellular ROS production. ROS was reported to promote HIF-1α accumulation by the inhibition of PHD catalytic activity via the oxidization of PHD-bound Fe^{2+} (Koivunen et al. 2007; Pan et al. 2007). However, it has been noted that a paradox exists between them, because the HIF-1α-dependent transcriptional program can prevent mitochondrial ROS generation (Jain et al. 2016). It is unclear whether MeHg-induced toxicity is associated with the expression of HIF-1α, whereas the specific relationship between ROS production and HIF-1α also remains unclear. MeHg predominantly accumulates in the CNS, particularly in astrocytes; the latter have been shown to play an important role in mediating MeHg-induced neurotoxicity (Ceccatelli et al. 2010; Shanker et al. 2003), inhibit glutamate uptake, and contribute to secondary excitotoxicity (Aschner et al. 2000; Deng et al. 2014; Liu et al. 2013, 2014). Astrocytes perform diverse important functions in providing support and nutrition (Abbott 2002; Rudge et al. 1994), inducing neuronal differentiation (Barkho et al. 2006) and mediating immune responses (Aschner 1998a, 1998b; Jensen et al. 2013). Therefore, we aimed to investigate the role of HIF-1α in MeHg-induced acute neurotoxicity by using primary rat astrocytes and adult rats, with special emphasis on an ROS mode of toxicity, so as to further identify novel therapeutic targets against MeHg-induced neuronal injury.

Materials and Methods

Primary Rat Astrocyte Isolation and Culture

Sprague-Dawley (SD) rats at the 1–2-d postnatal stage were purchased from the Laboratory Animal Center of Jiangsu University. Primary neonatal rat astrocytes were prepared as previously described (Bai et al. 2015, 2016; Fang et al. 2016; Yang et al. 2018; Yin et al. 2011). The procedures were as follows: Rats were rapidly decapitated, and the cerebral hemispheres were quickly obtained and rinsed with 4°C phosphate buffered solution (PBS). After dissecting away part of the meninges, basal ganglia, midbrain, and blood vessels, the remaining cortical tissues were cut into 1 mm^3 pieces and dissociated with 0.25% trypsin (Gibco) for 15 min at room temperature in the absence of stirring. Cells were grown in Dulbecco's Modified Eagle Medium (DMEM; Hyclone) containing 10% fetal bovine serum (Gibco), and 1% penicillin/streptomycin (Gibco). Culture medium was replaced with fresh medium twice a week, and cultures were maintained in a 5% CO_2 environment at 37°C. Cultured cells were used for experiments when astrocytes reached 75%–85% confluency. Protocols were approved by the Animal Ethics Committee of Jiangsu University of China and were carried out in accordance with the established Guiding Principles for Animal Research.

Reagents and Antibodies

Methylmercuric chloride (MeHgCl; Sigma-Aldrich) was dissolved in PBS to form a stock concentration of 10 mM; MG132; 3,4-Dihydroxybenzoic acid (DHB); cobalt chloride ($CoCl_2$); *N*-acetyl-cysteine (NAC) and Trolox (6-hydroxy-2,5,7,8-tetramethylchroman-2-carboxylic acid); and 3-(4,5-dimethylthiazol-2-yl)-2,5-diphenyl diphenyltetrazolium bromide (MTT)] were obtained from Sigma-Aldrich. Cycloheximide (CHX) was purchased from MedChemExpress; 2-methoxyestradiol (2-MeOE2) was purchased from Selleck Chemicals. For Western blotting analysis, the primary polyclonal antibodies to HIF-1α, VEGF-A, GLUT-1, and EPO were obtained from ImmunoWay, and antibodies to HIF-1β and β-actin were obtained from Cell Signaling Technology and CMATAG, respectively. Secondary antibodies used for immunoblotting included horseradish peroxidase (HRP)-conjugated antimouse (Santa Cruz Biotechnology) or anti-rabbit antibodies (Santa Cruz Biotechnology).

Cell Treatment

Astrocytes were treated for 0.5 h with MeHg at concentrations of 1.0, 2.5, 5.0, or 10 μM in the medium, and the cells treated by culture medium without MeHg were used as the control group. These concentrations were used in previous studies (Allen et al. 2001; Shapiro and Chan 2008). H_2O_2 (6 μM, 0.5 h), CHX (400 μM, 0.5, 1, or 2 h), MG132 (1 μM, 24 h), DHB (1 mM, 6 h), $CoCl_2$ (200 μM, 0.5 h), 2-MeOE2 (10 μM, 0.5 h), and NAC (2.5 mM, 4 h) or Trolox (2.5 mM, 4 h) were administered prior to MeHg treatment.

Cell Proliferation Assay

Cell proliferation was measured in astrocytes cultured in 96-well plates (1×10^4/well) using the MTT assay. At the end of treatment, MTT was added to each well at a final concentration of 0.5 mg/mL and incubated at 37°C for 4 h. Next, the MTT solution was replaced with dimethyl sulfoxide (150 μL/well) for 10 min to dissolve the dark-blue formazan crystals in intact cells, and the absorbance was measured at 490 nm with a Bio-Rad 680 Microplate Reader (Bio-Rad Laboratories).

Lactate Dehydrogenase (LDH) Release Assay

Cytotoxicity was detected using an LDH release assay kit (Jiancheng Bioengineering Institute of Nanjing) according to the manufacturer's protocol. Cells were cultured in 96-well plates (1×10^4/well), and after treatment supernatants were transferred

to clean 96-well plates. Absorbance was analyzed at 450 nm using a Bio-Rad 680 Microplate Reader.

Measurement of Intracellular ROS Generation

To measure ROS generation, a fluorometric assay was carried out using the cell membrane permeable dye 2′,7′-dichlorofluorescin diacetate (DCFH-DA). In the quantitative experiment of fluorescence intensity, cells cultured in 96-well plate (1×10^4/well) were treated with different concentrations of MeHg (1, 2.5, 5, and 10 μM) for 0.5 h and were then incubated with 10 μmol/L DCFH-DA in serum-free medium for 0.5 h at 37°C. After washing with PBS, the fluorescence intensity was measured with Cytation™ 5 (Biotek), with an excitation wavelength of 488 nm and an emission wavelength of 525 nm. In the imaging experiment, cells cultured in 24-well plates (5×10^4/well) were treated with MeHg (10 μM, 0.5 h) or H_2O_2 (6 μM, 0.5 h). After washing with PBS, the nuclei were stained with 4′,6-diamidino-2-phenylindole (DAPI) for 15 min at room temperature. Then the cells were incubated with 10 μmol/L DCFH-DA in serum-free medium for 0.5 h at 37°C. Finally, the resulting fluorescence was detected with a fluorescence microscope (Zeiss Axio Observer). Cells treated with H_2O_2 were used as the positive control. The intensity of fluorescence reflects the extent of oxidative stress.

Western Blotting Analysis

To prepare the whole protein lysate, cells were washed three times with cold PBS, lysed in lysis buffer (RIPA lysis buffer containing 1% PMSF, obtained from Beyotime), incubated on ice for 15 min, and collected after $12{,}000\times g$ centrifugation at 4°C for 15 min. The protein concentration was determined by a BCA protein assay reagent kit (Beyotime). A total of 60 μg of cell total protein was separated using 10% or 12% SDS-PAGE, then transferred to a PVDF membrane (Millipore). After being blocked with 5% skim milk in TBST (10 mM Tris–HCl, 120 mM NaCl, 0.1% Tween® 20, pH 7.4) for 2 h at room temperature, the membranes were incubated with specific primary antibodies overnight at 4°C (Table 1). On the second day, the membranes were washed three times with TBST buffer and further incubated with HRP-labeled secondary antibodies at room temperature for 1 h, and then washed three times in TBST. Finally, signal density of the immunoblots was performed using the MiniChemi Mini Size Chemiluminescent Imaging System (Beijing Sage Creation Science Co., Ltd.) and analyzed with Image J software (National Institutes of Health).

Adenovirus-Mediated HIF-1α Overexpression

Adenovirus carrying the HIF-1α gene was obtained from Hanbio Biotechnology Co., Ltd. Astrocytes were seeded in 6-well plates at a 60% confluence, and cells were transfected with pHBAd-EF1-MCS-GFP according to multiplicity of infection (MOI) = 30×10^8PFU/mL 8 h later, cells were supplemented with fresh medium and continuously cultured for an additional 48 h to observe transfection efficiency by means of Western blotting.

siRNA Transfection

The small interfering RNAs (siRNAs) for HIF-1α were designed and purchased from Guangzhou Ribobio Co., Ltd. The sequences of the three siRNAs were as follows:

#1 (siB07514101244) 5′-TCGACAAGCTTAAGAAAGA dTdT-3′,

#2 (siB07514101312) 5′-GGACAATATAGAAGACATT dTdT-3′ and

#3 (siG081230140326) 5′-CTGATAACGTGAACAAATA dTdT-3′.

Astrocytes were plated in 6-well plates at 60% confluence, transfected with HIF-1α siRNA (50 nM), or a negative control (NC, a scrambled sequence) siRNA (50 nM) with Lipofectamine®2000 in Opti-MEM medium (Invitrogen), according to the manufacturer's protocol. The transfected cells were incubated at 37°C for an additional 48 h and validated the silencing efficacy via Western blotting analysis.

Total RNA Extraction and Quantitative Real-Time PCR (RT-PCR)

Total RNA was extracted from astrocytes using the TRIzol reagent (Invitrogen). Five hundred nanograms of total RNA were reverse-transcribed to cDNA using an RT reagent kit (TaKaRa), which was then amplified with SYBR green dye on a CFX96 Real-Time PCR Detection System (Bio-Rad). The relative quantification of mRNA levels was calculated using the standard $2^{-\Delta\Delta Ct}$ relative quantification method.

The primers for rat HIF-1α and β-actin were designed and synthesized by Shanghai Generay Biotech Co., Ltd (Shanghai, China), and the sequences were as follows:

HIF-1α:
Forward primer: 5′-TCACAAATCAGCACCAAGCAC-3′
Reverse primer: 5′-AAGGGGAAAGAACAAAACACG-3′
β-actin:
Forward primer: 5′-CCTAGACTTCGAGCAAGAGA-3′
Reverse primer: 5′-GGAAGGAAGGCTGGAAGA-3′.

Animal Model

Male SD rats (8 wk old) weighing 200 ± 20 g were obtained from the Laboratory Animal Center of Jiangsu University (Accreditation Number: SCXK [SU] 2018-0012). The rats were housed in a temperature- and humidity-controlled room (22 ± 2°C and 50 ± 10% relative humidity) with a 12 h:12 h light:dark cycle (dark phase from 1900 to 0700) and were maintained on standard laboratory chow with ad libitum access to water and food ($n=6$ per cage). The rats were acclimatized for at least 7 d prior to MeHg exposure.

Rats were divided randomly into six groups ($n=6$):

Group I: Normal saline was injected intraperitoneally for 0.5 h

Table 1. Protein antibodies used for Western blotting.

Antibodies	Source	Catalog no.	Lot	Dilution
HIF-1α	ImmunoWay	YT2133	B3301	1:1,000
HIF-1β	Cell Signaling Technology	D28F3	2	1:1,000
GLUT-1	ImmunoWay	YT1928	B2801	1:1,000
EPO	ImmunoWay	YM0237	B3701	1:1,000
VEGF-A	ImmunoWay	YT5108	B0801	1:1,000
β-actin	CMCTAG	AT0048	380436SB	1:10,000
Mouse antirabbit IgG-HRP	Santa Cruz Biotechnology	sc-2357	K0718	1:10,000
m-IgGκ BP-HRP	Santa Cruz Biotechnology	sc-516102	E2318	1:10,000

Group II: MeHg [2 mg/kg body weight (BW)] was injected intraperitoneally for 0.5 h

Group III: MeHg (4 mg/kg BW) was injected intraperitoneally for 0.5 h

Group IV: MeHg (6 mg/kg BW) was injected intraperitoneally for 0.5 h

Group V: MeHg (8 mg/kg BW) was injected intraperitoneally for 0.5 h

Group VI: MeHg (10 mg/kg BW) was injected intraperitoneally for 0.5 h

At the end of the exposure period, the rats were anesthetized by intraperitoneal (IP) injection of pentobarbital to alleviate any potential discomfort and pain. Next, the brain cortices were rapidly frozen in liquid nitrogen and transferred to a –80°C freezer. All experimental procedures were conducted following a protocol approved by the Animal Care and Use Committee and Animal Ethics Committee of Jiangsu University (Accreditation Number: SYXK [SU] 2013-0036). All animals used in this study were treated humanely according to the institutional guidelines, with full consideration for the alleviation of distress and discomfort.

Statistical Analysis

All data are presented as the mean ± standard deviation (SD). All assays were repeated at least three times with at least three independently derived astrocyte cultures. Statistical significance was assessed by analysis of variance (ANOVA) with correction for multiple comparisons in post hoc analysis. CHX treatment assay was analyzed by a two-way ANOVA with Dunnett's post hoc test. Other multiple comparisons were analyzed by one-way ANOVA with Dunnett's or Tukey's post hoc test. All statistical analyses were performed using GraphPad Prism software. A p value of <0.05 was considered to be statistically significant.

Results

Effects of Methylmercury on Astrocyte Proliferation, Cytotoxicity, and Production of ROS

To investigate the effects of MeHg on cell proliferation and cytotoxicity in astrocytes, we incubated astrocytes with this organometal (0–10 μM) for 0.5 h. The MTT assay and LDH leakage were subsequently assessed. As shown in Figure 1A, compared with control cells, those treated with MeHg exhibited lower cell proliferation, which appeared to be concentration-dependent. MeHg treatment significantly increased LDH release in astrocytes, especially at concentrations of 5 and 10 μM (Figure 1B). Exposure to MeHg (5 and 10 μM, 0.5 h) induced a ∼1.6-fold increase in astrocytic LDH release compared with controls ($p < 0.05$). Next, we analyzed the effects of MeHg on ROS production by 2′,7′-dichlorofluorescin diacetate (DCFH-DA) fluorescence. As is shown in Figure 1C, MeHg at 5 and 10 μM caused a significant increase in ROS formation. Additionally, fluorescence images also showed that the fluorescence intensity of ROS was obviously enhanced in MeHg (10 μM, 0.5 h) group (Figure 1D).

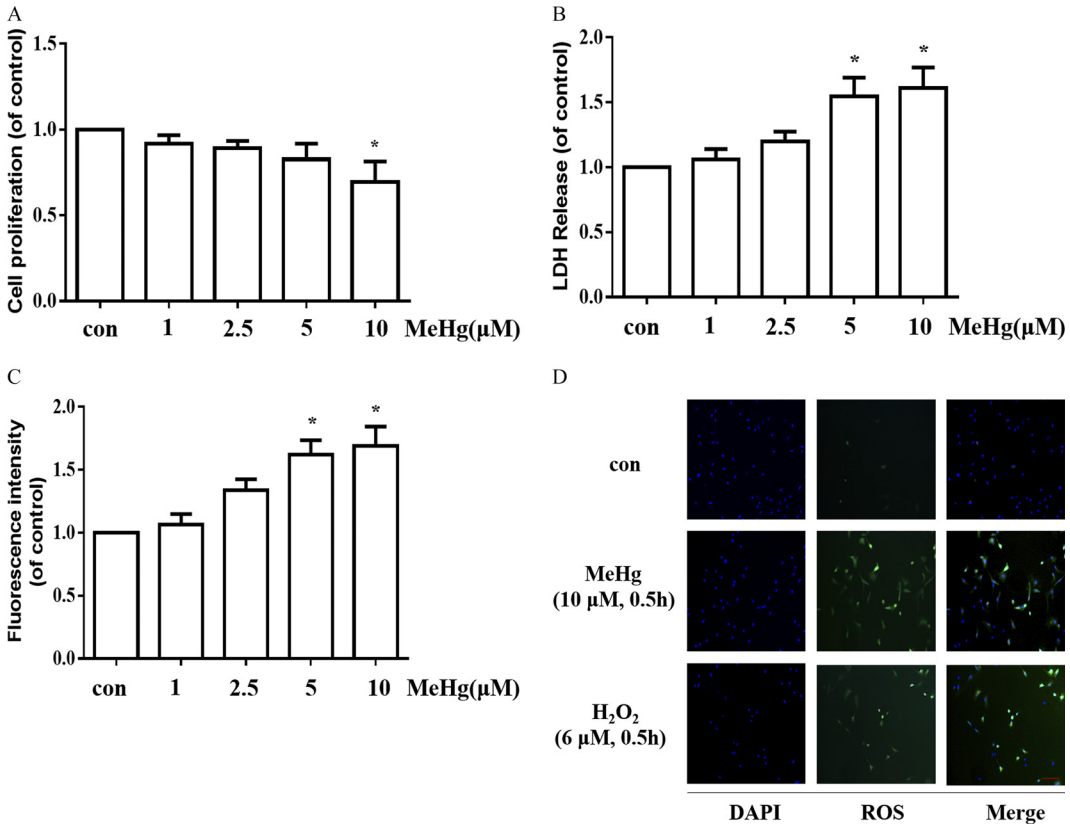

Figure 1. Cell proliferation, cytotoxicity and ROS production after treatment with MeHg for 0.5 h in astrocytes. (A) Cell proliferation in astrocytes was measured using the MTT assay. (B) Cytotoxicity in astrocytes was detected via LDH release. (C) Effects of MeHg treatment on ROS production using the fluorescent probe DCFH-DA. The fluorescence intensity was detected by the microplate reader. (D) Representative images for ROS generation induced by MeHg (10 μM, 0.5 h) treatment. Scale bar = 100 μm. H_2O_2 (6 μM, 0.5 h) was set as a positive control for ROS generation. Green fluorescence indicates ROS and blue (DAPI) indicates the nucleus. Note: Data are presented as mean ± SD from three independent experiments ($n = 3$). con, control (culture medium treatment without MeHg); DAPI, 4′,6-diamidino-2-phenylindole; DCFH-DA, 2′,7′-dichlorofluorescin diacetate; H_2O_2, hydrogen peroxide; LDH, lactate dehydrogenase; MeHg, methylmercury; MTT, 3-(4,5-dimethylthiazol-2-yl)-2,5-diphenyl diphenyltetrazolium bromide; ROS, reactive oxygen species. $^*p < 0.05$ vs. control by one-way analysis of variance (ANOVA) with Dunnett's post hoc test.

Effects of Methylmercury on the Expression of HIF-1α-Related Proteins in Astrocytes

We incubated astrocytes in the absence or presence of MeHg (1–10 μM) for 0.5 h and assessed HIF-1α and HIF-1β expression by Western blotting. MeHg-treated astrocytes exhibited a significant reduction in HIF-1α expression in a concentration-dependent manner (Figure 2A). In contrast, HIF-1β remained unaffected irrespective of the MeHg concentration (Figure 2B). Next, we analyzed the expression of HIF-1α targets (GLUT-1, EPO, and VEGF-A) in astrocytes treated with various concentrations of MeHg. A significant decrease in the expression of GLUT-1, EPO, and VEGF-A proteins was observed in astrocytes treated with 10 μM MeHg for 0.5 h ($p < 0.05$) (Figure 2C). These results are consistent with the ability of MeHg to decrease astrocytic HIF-1α levels, followed by a decrease in, GLUT-1, EPO, and VEGF-A expression.

Effects of Protein Synthesis, Proteasome, and PHD Inhibitors on Protein Expression of HIF-1α and Downstream Effectors in Methylmercury-Treated Astrocytes

To determine the means by which MeHg regulated HIF-1α expression, we analyzed the expression of the HIF-1α gene with RT-PCR. As shown in Figure 3A, MeHg pretreatment did not affect HIF-1α mRNA levels. Therefore, we further explored the potential causes of the significant reduction in HIF-1α levels caused by MeHg in astrocytes. CHX is a broad-spectrum and nonspecific protein synthesis inhibitor, and astrocytes were harvested after CHX pretreatment (400 μM) for 0.5, 1, and 2 h with and without MeHg treatment (10 μM, 0.5 h). In addition, MeHg treatment alone group (10 μM for 0.5, 1, and 2 h) was also established. Then, HIF-1α protein expression was analyzed (Figure 3B). In comparison with the control group, the protein level of HIF-1α in CHX alone group decreased in a time-dependent manner. Notably, when compared with the corresponding time point of CHX treatment alone group, the level of HIF-1α protein was found to be significantly lower in the CHX + MeHg group ($p < 0.05$, Figure 3B). We pretreated astrocytes with or without MG132 (1 μM, 24 h), a proteasome inhibitor, followed by 10 μM MeHg, and incubated the cells for an additional 0.5 h. The cells were harvested at the end of the treatment, and the levels of HIF-1α and its targets were measured via Western blotting. As shown in Figure 3C, MG132 treatment inhibited the significant MeHg-induced reduction in HIF-1α and its target proteins in astrocytes. Previous research has suggested that HIF-1α degradation is attributable to the activation of proline hydroxylase (PHD)

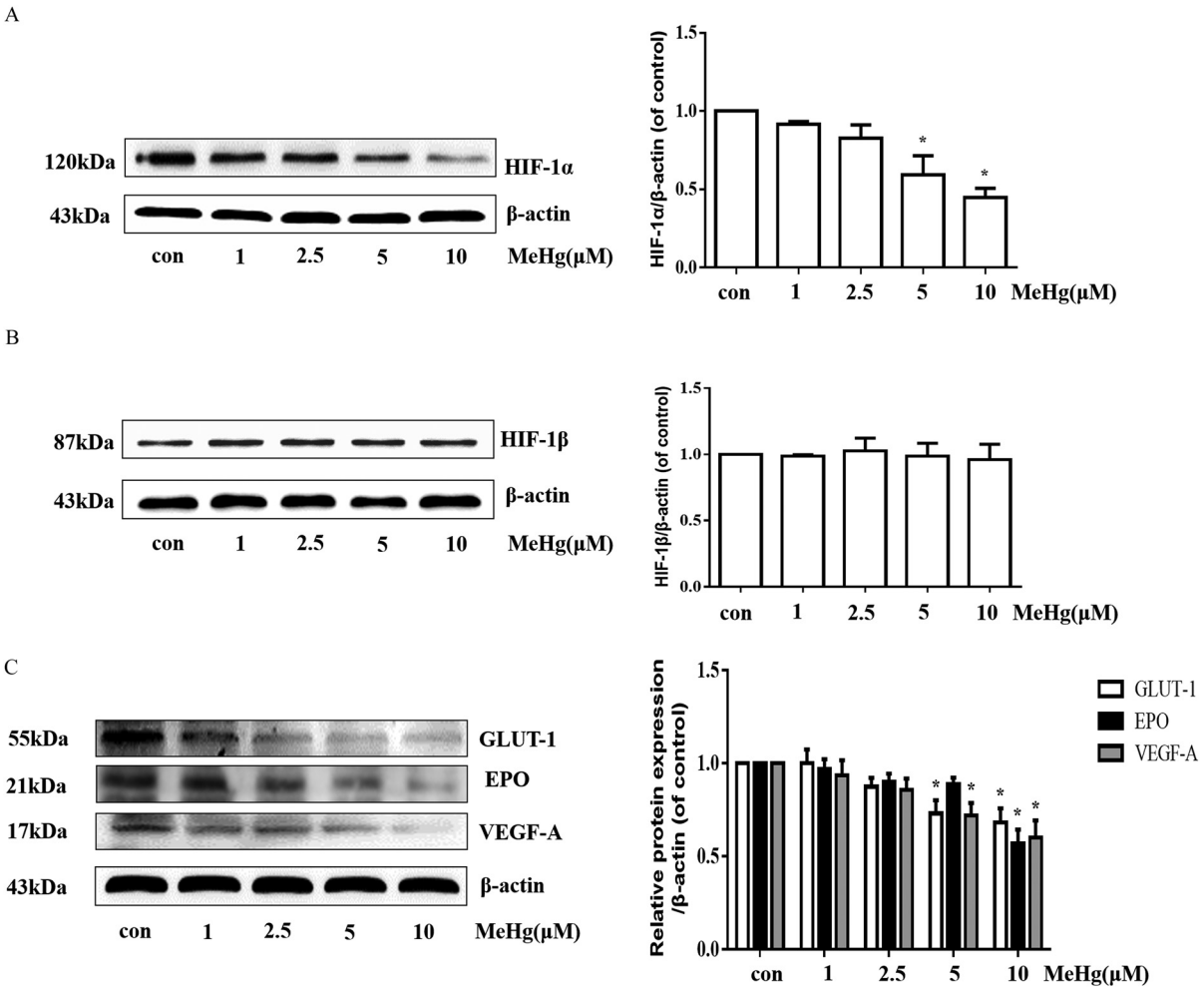

Figure 2. Effects of MeHg on the expression of HIF-1α–related proteins in astrocytes. (A) Western blotting for HIF-1α in astrocytes following MeHg (0, 1, 2.5, 5 or 10 μM, 0.5 h) exposure. (B) Western blotting for HIF-1β in astrocytes following MeHg (0, 1, 2.5, 5, or 10 μM, 0.5 h) exposure. (C) Effect of MeHg (0, 1, 2.5, 5, or 10 μM, 0.5 h) exposure on the expression of the downstream proteins of HIF-1α, including GLUT-1, EPO, and VEGF-A. β-actin was used as the internal control. Note: Data are presented as mean ± SD from three independent experiments ($n = 3$). con, control (culture medium treatment without MeHg); EPO, erythropoietin; GLUT-1, glucose transporter 1; HIF-1α, Hypoxia-inducible factor-1α; HIF-1β, Hypoxia-inducible factor-1β; MeHg, methylmercury; VEGF-A, vascular endothelial growth factor A. $^{*}p < 0.05$ vs. control by one-way ANOVA with Dunnett's post hoc test.

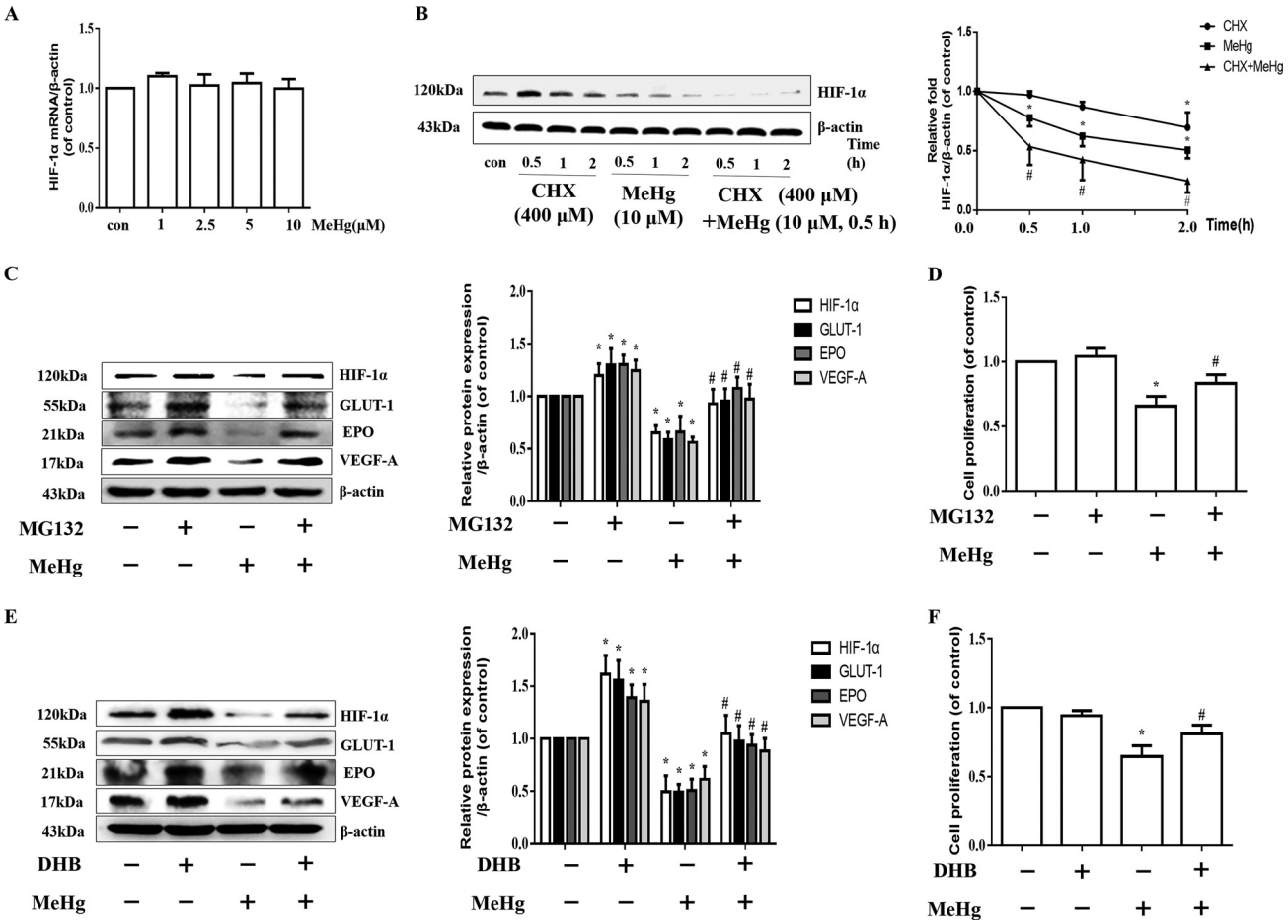

Figure 3. Effects of protein expression of HIF-1α and its downstream effectors and effects on cell proliferation induced by CHX, MG132, or DHB in MeHg-treated astrocytes. (A) Astrocytes were treated with MeHg (0, 1, 2.5, 5, or 10 μM, 0.5 h) and HIF-1α mRNA was evaluated. mRNA was normalized to β-actin and plotted relative to the control. $^{*}p < 0.05$ vs. the control by one-way ANOVA with Dunnett's post hoc test. (B) Cells were pretreated with 400 μM CHX for 0.5, 1 and 2 h and then exposed to 10 μM MeHg for 0.5 h. MeHg treatment alone group (10 μM for 0.5, 1 and 2 h) was also established. HIF-1α protein levels were analyzed by western blotting. β-actin was used to normalize the protein level and the intensities were presented as fold changes relative to the control. $^{*}p < 0.05$ vs. the control by one-way ANOVA with Dunnett's post hoc test. $^{\#}p < 0.05$ the CHX + MeHg group vs. the corresponding time point of CHX alone group by two-way ANOVA with Dunnett's post hoc test. (C) Cells were pretreated with MG132 (1 μM, 24 h) and then treated with 10 μM MeHg for 0.5 h. Western blotting was used to evaluate protein levels of HIF-1α, GLUT-1, EPO, and VEGF-A. (D) Effect of MG132 (1 μM, 24 h) on the cell proliferation was evaluated using an MTT assay. (E) Effect of DHB pretreatment (1 mM, 6 h) on the expression of HIF-1α, GLUT-1, EPO, and VEGF-A was detected by western blotting. (F) Effect of DHB pretreatment (1 mM, 6 h) on the cell proliferation was determined by an MTT assay. For Western blotting analyses, β-actin was used to normalize the protein level. Note: Statistical analysis was performed by one-way ANOVA with Tukey's post hoc test. Data are presented as mean ± SD from three independent experiments ($n = 3$). CHX, cycloheximide; con, control (culture medium treatment without MeHg); DHB, 3,4-Dihydroxybenzoic acid; EPO, erythropoietin; GLUT-1, glucose transporter 1; HIF-1α, Hypoxia-inducible factor-1α; MeHg, methylmercury; MG132, proteasome inhibitor; MTT, 3-(4,5-dimethylthiazol-2-yl)-2,5-diphenyl diphenyltetrazolium bromide; VEGF-A, vascular endothelial growth factor A. $^{*}p < 0.05$ vs. control, $^{\#}p < 0.05$ vs. MeHg only-group.

(Marxsen et al. 2004). To define the potential contribution of PHD-mediated inhibition of HIF-1α in response to MeHg treatment, we treated astrocytes with 1 mM DHB [a small-molecule prolyl hydroxylase (PHD) inhibitor] (Siddiq et al. 2005) for 6 h and exposed astrocytes to 10 μM MeHg for 0.5 h. Notably, compared with cells treated with MeHg alone, astrocytic HIF-1α expression in cells treated with MeHg and either the proteasome inhibitor (Figure 3C) or the PHD inhibitor (Figure 3E) was significantly higher. In addition, both the proteasome inhibitor and PHD inhibitor restored MeHg-inhibited cell proliferation (Figure 3D and 3F).

Effects of Pharmacologic and Genetic Manipulation of HIF-1α on Cell Proliferation

We hypothesized that decreased HIF-1α protein contributes to astrocytic cytotoxicity. To further confirm this hypothesis, we treated astrocytes with $CoCl_2$ (200 μM, 0.5 h) or 2-MeOE2 (10 μM, 0.5 h) in the absence or presence of MeHg (0.5 h exposure). We used $CoCl_2$, an inducer of HIF-1α expression (Triantafyllou et al. 2006), and 2-MeOE2, a HIF-1α inhibitor (Chen et al. 2008; Parada-Bustamante et al. 2015; Pribluda et al. 2000), to regulate HIF-1α expression in MeHg-treated astrocytes (Figure 4A and 4C). Analogous to the data shown in Figure 3D and 3F, overexpression of HIF-1α protein mitigated the MeHg-reduced cell proliferation in astrocytes ($p < 0.05$) (Figure 4B), whereas down-regulation of HIF-1α protein significantly aggravated the decline in astrocytic proliferation caused by MeHg ($p < 0.05$) (Figure 4D). To confirm this observation, we further used siRNA and adenovirus overexpression, which target the HIF-1α gene (Figure 4E to 4H). Consistent with the results of $CoCl_2$ and 2-MeOE2 treatment, overexpression of HIF-1α significantly attenuated the decline in MeHg-

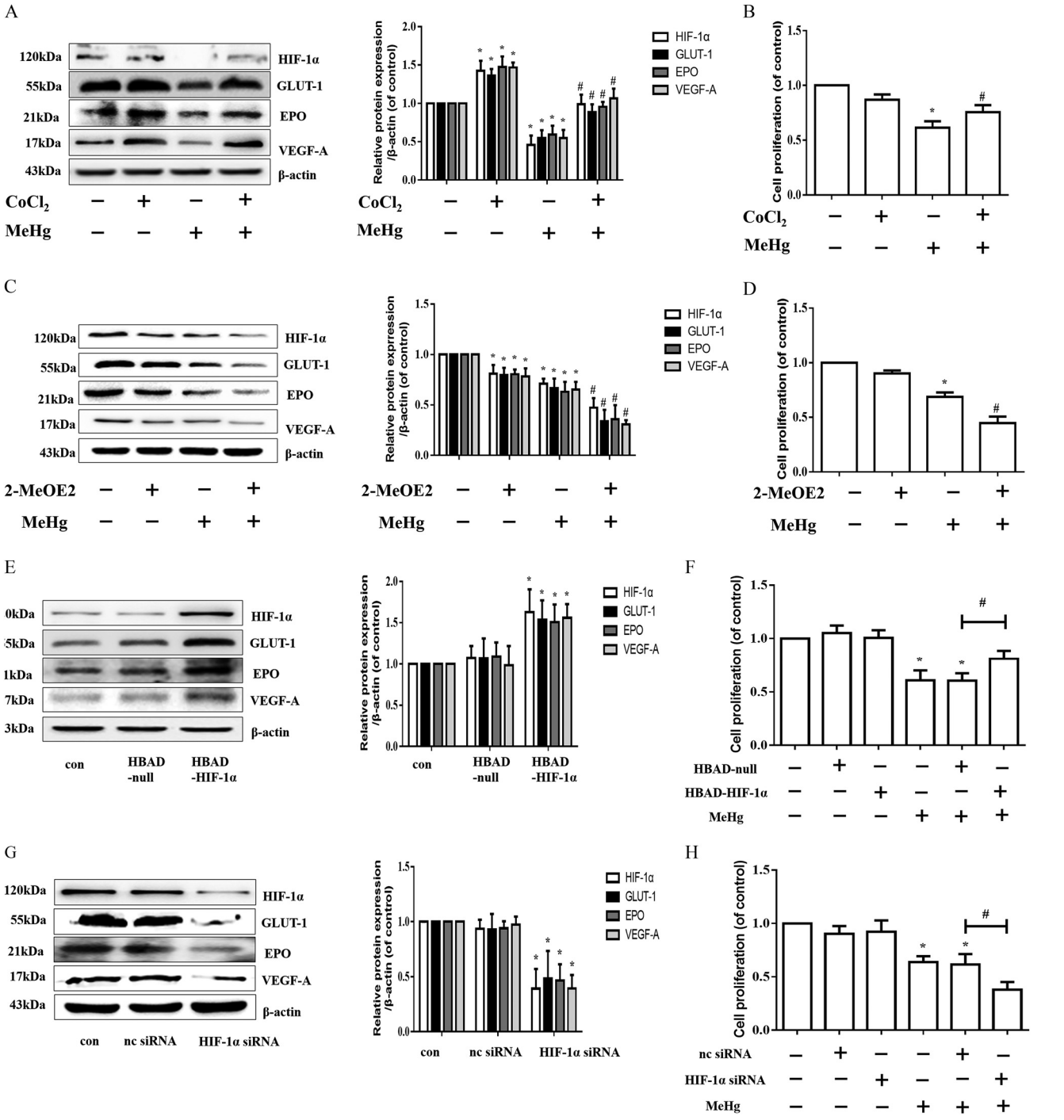

Figure 4. Effects of pharmacologic and genetic manipulation of HIF-1α on cell proliferation. (A) Astrocytes were pretreated with $CoCl_2$ (200 μM, 0.5 h) and then treated with 10 μM MeHg for 0.5 h. Western blotting was used to evaluate protein levels of HIF-1α, GLUT-1, EPO, and VEGF-A. (B) Effect of $CoCl_2$ pretreatment (200 μM, 0.5 h) on the cell proliferation was evaluated using an MTT assay. (C) Effect of 2-MeOE2 pretreatment (10 μM, 0.5 h) on the expression of HIF-1α, GLUT-1, EPO, and VEGF-A was detected by Western blotting. (D) Effect of 2-MeOE2 pretreatment (10 μM, 0.5 h) on the cell proliferation was evaluated using an MTT assay. For Western blotting analyses, representative blots are shown, and the intensities are presented as fold changes relative to the control group (β-actin as the internal control). $^{*}p < 0.05$ vs. control, $^{\#}p < 0.05$ vs. MeHg-only group. (E) The protein expression levels of HIF-1α, GLUT-1, EPO, and VEGF-A after overexpression of HIF-1α. $^{*}p < 0.05$ vs. HBAD-null group. (F) Effect of adenovirus-induced HIF-1α overexpression on the decrease in MeHg-induced cell proliferation as determined by an MTT assay. $^{*}p < 0.05$ vs. control group, $^{\#}p < 0.05$ vs. MeHg + HBAD-null group. (G) Effect of HIF-1α siRNA on the protein expression of HIF-1α, GLUT-1, EPO, and VEGF-A. (H) Effect of HIF-1α siRNA on the MeHg-induced decrease in cell proliferation. Note: Statistical analysis was performed by one-way ANOVA with Tukey's post hoc test. Data are presented as the mean ± SD from three independent experiments ($n = 3$). $CoCl_2$, cobalt chloride; con, control (culture medium treatment without MeHg); EPO, erythropoietin; GLUT-1, glucose transporter 1; HBAD, pHBAd-EF1-MCS-GFP; HIF-1α, Hypoxia-inducible factor-1α; 2-MeOE2, 2-methoxyestradiol; MeHg, methylmercury; MTT, 3-(4,5-dimethylthiazol-2-yl)-2,5-diphenyl diphenyltetrazolium bromide; nc siRNA, negative control (scrambled sequence) siRNA; siRNA, small interfering RNA; VEGF-A, vascular endothelial growth factor A. $^{*}p < 0.05$ vs. nc siRNA group. $^{*}p < 0.05$ vs. control group, $^{\#}p < 0.05$ vs. MeHg + nc siRNA group.

induced cell proliferation (Figure 4F), whereas inhibition of HIF-1α significantly increased the decline in cell proliferation (Figure 4H; $p < 0.05$).

HIF-1α Protein Expression and Cell Proliferation after Pretreatment with Antioxidants in Methylmercury-Treated Astrocytes

We investigated whether ROS production were associated with decreased HIF-1α expression in MeHg-exposed astrocytes. Astrocytes were pretreated with NAC (2.5 mM, 4 h) and Trolox (2.5 mM, 4 h) followed by 10 μM MeHg for 0.5 h. NAC and Trolox are antioxidants that are commonly used to mitigate ROS (Aremu et al. 2008; Bai et al. 2015; Kaur et al. 2010). As shown in Figures 5A and 5C, cells pretreated with either NAC or Trolox and then treated with MeHg exhibited higher HIF-1α protein levels, similar to those of control cells, than those treated with MeHg alone. Pretreated cells exhibited higher levels (as much as ~30%) of cell proliferation than those treated with MeHg alone ($p < 0.05$) (Figure 5B and 5D).

Protein Expression of HIF-1α and Downstream Effectors following MeHg Administration in in Vivo *Rat Models*

Finally, to evaluate the *in vivo* effects of MeHg on HIF-1α protein expression, we established a SD rat model. Animals were administered with MeHg (0, 2, 4, 6, 8, and 10 mg/kg, each group with 6 rats) by intraperitoneal injection and sacrificed 0.5 h later. The expression of HIF-1α and its target proteins in brain tissues was measured by Western blotting. As shown in Figure 6, MeHg treatment significantly decreased the expression of HIF-1α and its targets, especially in rats exposed to 8 mg/kg and 10 mg/kg MeHg ($p < 0.05$).

Discussion

In the present study, we report that, compared with the vehicle control, treatment with 5 or 10 μM MeHg for 0.5 h resulted in lower cell proliferation and higher ROS generation in primary rat astrocytes, and these results were associated with lower expression of HIF-1α. To define the mechanism(s) of the MeHg-induced alteration in HIF-1α expression, first we detected the mRNA level of HIF-1α after MeHg treatment. The results showed that MeHg exposure resulted in a significant reduction in HIF-1α levels without affecting HIF-1α transcription. Then, we speculated that whether MeHg affected the degradation of HIF-1α protein. The results showed that treating cells with CHX + MeHg results in lower protein expression of HIF-1α than does treating cells with CHX alone in three different time points. Because CHX blocks protein synthesis, it would stand to reason that the effect of MeHg in these cells is associated with protein degradation. Additionally, we also demonstrated that the proteasome inhibitor (MG132) and the PHD inhibitor (DHB), both of which block protein degradation of HIF-1α, partially restored the inhibitory effect of MeHg on HIF-1α protein, further suggesting that the MeHg-induced decrease in HIF-1α protein is due to the promoted degradation. Furthermore, taking advantage of genetic and pharmacological methods to alter inherent levels of the HIF-1α protein, we provide evidence directly linking MeHg toxicity with HIF-1α inhibition. It is noteworthy that lower HIF-1α protein expression was related to the production of ROS, as demonstrated by NAC and Trolox. Taken together, our

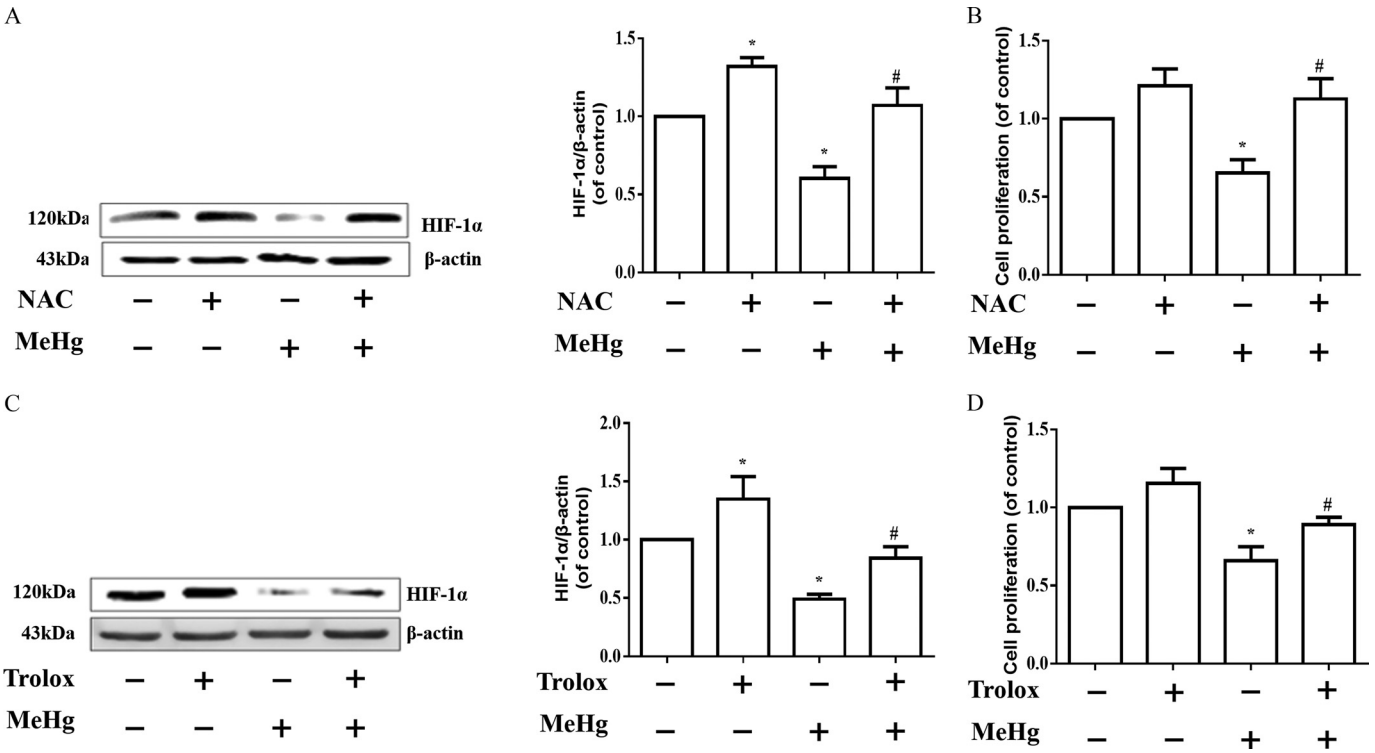

Figure 5. HIF-1α protein expression and cell proliferation after pre-treatment with antioxidants in MeHg-treated astrocytes. (A) Effect of NAC pretreatment (2.5 mM, 4 h) on HIF-1α protein expression. (B) Effect of NAC pretreatment on the decreased cell proliferation induced by MeHg. (C) Effect of Trolox pretreatment (2.5 mM, 4 h) on HIF-1α protein expression. (D) Effect of Trolox pretreatment on the MeHg-induced decrease in cell proliferation. Note: Statistical analysis was performed by one-way ANOVA with Tukey's post hoc test. Data are presented as the mean ± SD from three independent experiments ($n = 3$). con, control (culture medium treatment without MeHg); HIF-1α, Hypoxia-inducible factor-1α; MeHg, methylmercury; MTT, 3-(4,5-dimethylthiazol-2-yl)-2,5-diphenyl diphenyltetrazolium bromide; NAC, *N*-acetyl-cysteine, Trolox, 6-hydroxy-2,5,7,8-tetramethylchroman-2-carboxylic acid. $^{*}p < 0.05$ vs. control, $^{\#}p < 0.05$ vs. MeHg-only group.

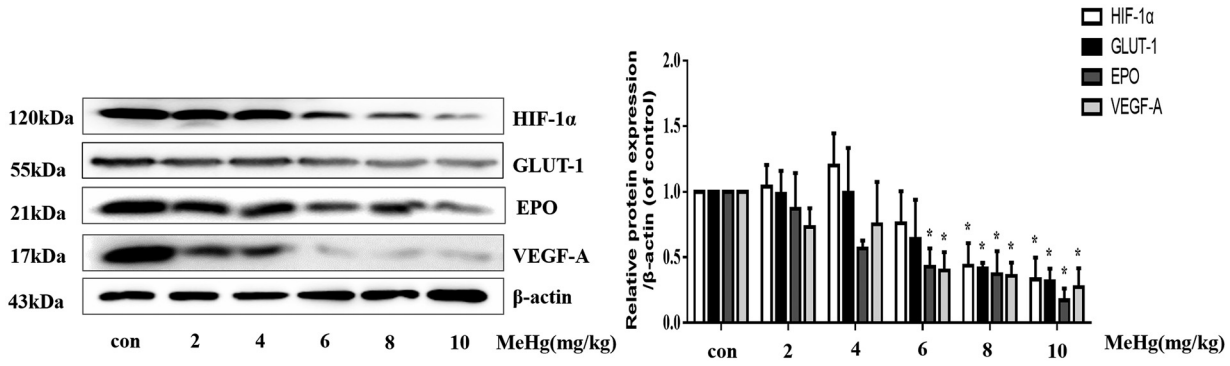

Figure 6. Protein expression of HIF-1α and downstream effectors following MeHg administration in *in vivo* rat models. Adult Sprague-Dawley rats were administered with MeHg (0, 2, 4, 6, 8, 10 mg/kg) by intraperitoneal injection for 0.5 h. Whole brain lysates were analyzed by Western blotting for the indicated proteins. Note: Data are presented as mean ± SD ($n = 6$ rats/group). con, control (intraperitoneal injection of saline); EPO, erythropoietin; GLUT-1, glucose transporter 1; HIF-1α, Hypoxia-inducible factor-1α; MeHg, methylmercury; VEGF-A, vascular endothelial growth factor A. $^{*}p < 0.05$ vs. control group by one-way ANOVA with Dunnett's post hoc test.

novel observations suggest that ROS act as an important regulator of HIF-1α inhibition in MeHg-treated astrocytes and that overexpression of HIF-1α may afford a novel neuroprotective effect in the treatment of MeHg-induced neurotoxicity. Moreover, we also found that MeHg inhibited the expression of HIF-1α in the SD rat brain, which better revealed the relationship between MeHg and the HIF-1α signaling pathway found in the *in vitro* and *in vivo* experiments.

MeHg is an established neurotoxicant (Aschner and Syversen 2005; Clarkson and Magos 2006; Culbreth and Aschner, 2016; Farina et al. 2011a, 2011b), whose mechanism(s) of toxicity have yet to be fully understood; however, oxidative stress seems to play a role (Aschner et al. 2007; Santos et al. 2018; Ishihara et al. 2016). Oxidative stress is one of the known mechanisms for the induction of HIF-1α. Previous studies have consistently shown that metals, such as lead (Das et al. 2015), aluminum (Mailloux and Appanna 2007), manganese (Han et al. 2009), and zinc (Pan et al. 2013; Park et al. 2018), as well as other xenobiotics, such as isoflurane (Cao et al. 2018; Sun et al. 2013), can increase HIF-1α expression. In contrast, concentration-dependent inhibition of HIF-1α in Hep3B cells has been reported in response to cadmium and inorganic mercury (Hg) treatment (Horiguchi et al. 2000).

We speculated that two factors contribute to the decreased level of HIF-1α protein in response to MeHg treatment. First, MeHg-induced mitochondrial damage might cause a reduction in oxygen consumption and increase relative oxygen content, leading to redistribution of oxygen and binding to PHD and an increase in PHD activity (Wu et al. 2010), whereas other metals, including inorganic mercury, mimicked a hypoxic state and induced pseudohypoxia to promote the translocation of HIF-1α (Mailloux and Appanna 2007). MeHg did not change the level of HIF-1α in brain microvascular pericytes (Hirooka et al. 2013). Second, MeHg might increase 2-oxoglutarate (2-OG) levels, a cofactor of PHD. 2-OG has been shown to increase PHD activity, resulting in increased degradation of HIF-1α and a net decrease in HIF-1α protein (Dehne et al. 2010; Mailloux et al. 2009; Matsumoto et al. 2006). As shown in Figure 3, MeHg appeared to have activated PHD and UPS, thus promoting HIF-1α degradation.

HIF-1α regulates the expression of a large number of genes that are involved in glucose metabolism, energy production, angiogenesis, migration, and other cellular processes (Liu et al. 2012; Semenza 2002). Thus, reduced availability of HIF-1α and the subsequent reduction in expression of its target genes may cause cellular dysfunction. VEGF-A, GLUT-1, and EPO are typical downstream target proteins of HIF-1α (Ashok et al. 2017; Cramer et al. 2003; Mense et al. 2006; Semenza 2002). VEGF-induced angiogenesis has previously been shown to improve the blood supply to neurons and slow the clinical deterioration in Alzheimer's disease (Bogaert et al. 2006). VEGF and EPO have been shown to improve tissue oxygen content by promoting erythropoiesis and angiogenesis, which may stimulate genes involved in glucose transport and metabolism (Ashok et al. 2017; Semenza 2002). It is noteworthy that HIF-1α complexes can regulate the biological functions of various genes, such as those involved in vascular growth, oxygen transport, and energy metabolism (Czibik 2010). Thus, we suggest that the mechanism of MeHg neurotoxicity involves, at least in part, a reduction in HIF-1α and its downstream proteins (GLUT-1, EPO, and VEGF-A), leading to secondary alterations in blood flow, tissue oxygenation, and ATP production. In addition, studies on the regulation of PHD have generated interest as investigational drugs for anemia and neurodegenerative diseases. The use of a small molecule of HIF-1α PHD inhibitor (FG-4592), has been promoted to clinical trials for treating anemia by increasing erythropoiesis through HIF-1α mediated transcription (Besarab et al. 2016; Chen et al. 2017; Haase 2017), as well as for treating Parkinson's disease by HIF-1α-targeted positive regulation of redox biology and mitochondrial function (Li et al. 2018). In the present study, the suppression of MeHg toxicity by both $CoCl_2$ and adenovirus-targeted HIF-1α overexpression suggested that activation of the HIF-1α pathway can reverse inhibition of cell proliferation by MeHg (Figure 4). Thus, we suggest that HIF-1α can be pursued as a novel target for MeHg poisoning.

MeHg-induced toxicity is mediated, at least in part, by oxidative stress (Polunas et al. 2011; Yee and Choi 1996). In addition, rapid degradation of HIF-1α may result from ROS generation (Beattie et al. 2005; Cairo et al. 1996; Henkel and Krebs 2004; Jaeckel et al. 2005; Li et al. 2006; Sato and Kondoh 2002). We initially considered that ROS generation could play a role in the altered HIF-1α protein expression to mediate MeHg toxicity. Treatment of rat astrocytes with oxygen radical scavengers (NAC and Trolox) resulted in higher HIF-1α protein expression and increased cell proliferation (Figure 5), suggesting that detoxification of ROS by HIF-1α is associated with its neuroprotective effects. Reductions in HIF-1α expression in MeHg-treated astrocytes and rats suggest that the up-regulation of HIF-1α affords neuroprotective effects. Taking into account the limitations of the pharmacological and genetic regulations of clinical toxicity and the ability of antioxidants to promote HIF-1α expression, the use of antioxidants should be considered for clinical detoxification. However, MeHg can affect many cellular and molecular functions if the MeHg exposure concentrations and duration are sufficient.

Thus, additional research on the toxicological significance of HIF-1α suppression by acute exposure to MeHg is warranted, in addition to a more precise delineation of its protective mechanisms.

In conclusion, we demonstrated that MeHg led to astrocytic neurotoxicity *in vitro* by reducing levels of HIF-1α and its downstream proteins, which may result from increasing PHD activity, which in turn promoted HIF-1α degradation. Furthermore, the up-regulation of HIF-1α imparted protection against MeHg neurotoxicity. Taken together, these findings—from both *in vivo* and *in vitro* experiments—suggest that HIF-1α may be as of yet an unrecognized and important mediator or regulator of MeHg-induced neurotoxicity, and this means of increasing HIF-1α activation in astrocytes may afford a therapeutic strategy for mitigating MeHg poisoning.

Acknowledgments

The authors are grateful to P. Spencer at Oregon Health & Science University, M. Ghert at McMaster University, and J. Cai at University of Oklahoma Health Science Center for their critical comments. This work was supported in part by the Natural Science Foundation of China (Nos. 30872139, 81273124, 31100964) and R01 ES07331, R01 ES10563, and ES020852 from the National Institute of Environmental Health Sciences (NIEHS).

References

Abbott NJ. 2002. Astrocyte-endothelial interactions and blood-brain barrier permeability. J Anat 200(6):629–638, PMID: 12162730, https://doi.org/10.1046/j.1469-7580.2002.00064.x.

Allen JW, El-Oqayli H, Aschner M, Syversen T, Sonnewald U. 2001. Methylmercury has a selective effect on mitochondria in cultured astrocytes in the presence of [U-13C] glutamate. Brain Res 908(2):149–154, PMID: 11454325, https://doi.org/10.1016/S0006-8993(01)02628-2.

Aremu DA, Madejczyk MS, Ballatori N. 2008. N-acetylcysteine as a potential antidote and biomonitoring agent of methylmercury exposure. Environ Health Perspect 116(1):26–31, PMID: 18197295, https://doi.org/10.1289/ehp.10383.

Aschner M. 1998a. Immune and inflammatory responses in the CNS: modulation by astrocytes. Toxicol Lett 102-103(3):283–287, PMID: 10022267, https://doi.org/10.1016/s0378-4274(98)00324-5.

Aschner M. 1998b. Astrocytes as mediators of immune and inflammatory responses in the CNS. Neurotoxicology 19(2):269–281, PMID: 9553964, https://doi.org/10.1016/s1383-5742(97)00039-2.

Aschner M, Syversen T. 2005. Methylmercury: recent advances in the understanding of its neurotoxicity. Ther Drug Monit 27(3):278–283, PMID: 15905795, https://doi.org/10.1097/01.ftd.0000160275.85450.32.

Aschner M, Syversen T, Souza DO, Rocha JB, Farina M. 2007. Involvement of glutamate and reactive oxygen species in methylmercury neurotoxicity. Braz J Med Biol Res 40(3):285–291, PMID: 17334523, https://doi.org/10.1590/s0100-879x2007000300001.

Aschner M, Yao CP, Allen JW, Tan KH. 2000. Methylmercury alters glutamate transport in astrocytes. Neurochem Int 37(2–3):199–206, PMID: 10812205, https://doi.org/10.1016/S0197-0186(00)00023-1.

Ashok BS, Ajith TA, Sivanesan S. 2017. Hypoxia-inducible factors as neuroprotective agent in Alzheimer's disease. Clin Exp Pharmacol Physiol 44(3):327–334, PMID: 28004401, https://doi.org/10.1111/1440-1681.12717.

Bai Y, Yin C, Zhao W, Li B, Qian H, Ma J, et al. 2015. Differential protection of pre-versus post-treatment with curcumin, Trolox, and N-acetylcysteine against acrylonitrile-induced cytotoxicity in primary rat astrocytes. Neurotoxicology 51:58–66, PMID: 26409646, https://doi.org/10.1016/j.neuro.2015.09.011.

Bai Y, Zhao W, Yin C, Fang Y, Ma J, Li B, et al. 2016. Preconditioning of endoplasmic reticulum stress protects against acrylonitrile-induced cytotoxicity in primary rat astrocytes: the role of autophagy. Neurotoxicology 55:112–121, PMID: 27260289, https://doi.org/10.1016/j.neuro.2016.05.020.

Barkho BZ, Song H, Aimone JB, Smrt RD, Kuwabara T, Nakashima K, et al. 2006. Identification of astrocyte-expressed factors that modulate neural stem/progenitor cell differentiation. Stem Cells Dev 15(3):407–421, PMID: 16846377, https://doi.org/10.1089/scd.2006.15.407.

Beattie JH, Owen HL, Wallace SM, Arthur JR, Kwun IS, Hawksworth GM, et al. 2005. Metallothionein overexpression and resistance to toxic stress. Toxicol Lett 157(1):69–78, PMID: 15795095, https://doi.org/10.1016/j.toxlet.2005.01.005.

Belletti S, Orlandini G, Vettori MV, Mutti A, Uggeri J, Scandroglio R, et al. 2002. Time course assessment of methylmercury effects on C6 glioma cells: submicromolar concentrations induce oxidative DNA damage and apoptosis. J Neurosci Res 70(5):703–711, PMID: 12424738, https://doi.org/10.1002/jnr.10419.

Berra E, Benizri E, Ginouvès A, Volmat V, Roux D, Pouysségur J. 2003. HIF prolyl-hydroxylase 2 is the key oxygen sensor setting low steady-state levels of HIF-1α in normoxia. EMBO J 22(16):4082–4090, PMID: 12912907, https://doi.org/10.1093/emboj/cdg392.

Besarab A, Chernyavskaya E, Motylev I, Shutov E, Kumbar LM, Gurevich K, et al. 2016. Roxadustat (FG-4592): correction of anemia in incident dialysis patients. J Am Soc Nephrol 27(4):1225–1233, PMID: 26494833, https://doi.org/10.1681/ASN.2015030241.

Bogaert E, Damme PV, Bosch LVD, Robberecht W. 2006. Vascular endothelial growth factor in amyotrophic lateral sclerosis and other neurodegenerative diseases. Muscle Nerve 34(4):391–405, PMID: 16856151, https://doi.org/10.1002/mus.20609.

Bruick RK, McKnight SL. 2001. A conserved family of prolyl-4-hydroxylases that modify HIF. Science 294(5545):1337–1340, PMID: 11598268, https://doi.org/10.1126/science.1066373.

Cairo G, Castrusini E, Minotti G, Bernelli-Zazzera A. 1996. Superoxide and hydrogen peroxide-dependent inhibition of iron regulatory protein activity: a protective stratagem against oxidative injury. FASEB J 10(11):1326–1335, PMID: 8836047, https://doi.org/10.1096/fasebj.10.11.8836047.

Canuel R, de Grosbois SB, Atikessé L, Lucotte M, Arp P, Ritchie C, et al. 2006. New evidence on variations of human body burden of methylmercury from fish consumption. Environ Health Perspect 114(2):302–306, PMID: 16451872, https://doi.org/10.1289/ehp.7857.

Cao Y, Li Z, Ma L, Ni C, Li L, Yang N, et al. 2018. Isoflurane-induced postoperative cognitive dysfunction is mediated by hypoxia-inducible factor-1α-dependent neuroinflammation in aged rats. Mol Med Rep 17(6):7730–7736, PMID: 29620198, https://doi.org/10.3892/mmr.2018.8850.

Carocci A, Rovito N, Sinicropi S, Genchi G. 2014. Mercury toxicity and neurodegenerative effects. In: *Reviews of Environmental Contamination and Toxicology. Reviews of Environmental Contamination and Toxicology (Continuation of Residue Reviews)*, vol 229. Whitacre D, eds. Cham, Switzerland: Springer, 1–18, PMID: 24515807, https://doi.org/10.1007/978-3-319-03777-6_1.

Carrasco L, Benejam L, Benito J, Bayona JM, Díez S. 2011. Methylmercury levels and bioaccumulation in the aquatic food web of a highly mercury-contaminated reservoir. Environ Int 37(7):1213–1218, PMID: 21658770, https://doi.org/10.1016/j.envint.2011.05.004.

Ceccatelli S, Daré E, Moors M. 2010. Methylmercury-induced neurotoxicity and apoptosis. Chem Biol Interact 188(2):301–308, PMID: 20399200, https://doi.org/10.1016/j.cbi.2010.04.007.

Chen W, Jadhav V, Tang J, Zhang JH. 2008. HIF-1 alpha inhibition ameliorates neonatal brain damage after hypoxic-ischemic injury. Acta Neurochir Suppl 102:395–399, PMID: 19388354, https://doi.org/10.1007/978-3-211-85578-2_77.

Chen N, Qian J, Chen J, Yu X, Mei C, Hao C, et al. 2017. Phase 2 studies of oral hypoxia-inducible factor prolyl hydroxylase inhibitor FG-4592 for treatment of anemia in China. Nephrol Dial Transplant 32(8):1373–1386, PMID: 28371815, https://doi.org/10.1093/ndt/gfx011.

Choi SM, Choi KO, Park YK, Cho H, Yang EG, Park H. 2006. Clioquinol, a Cu (II)/Zn (II) chelator, inhibits both ubiquitination and asparagine hydroxylation of hypoxia-inducible factor-1alpha, leading to expression of vascular endothelial growth factor and erythropoietin in normoxic cells. J Biol Chem 281(45):34056–34063, PMID: 16973622, https://doi.org/10.1074/jbc.M603913200.

Clarkson TW, Magos L. 2006. The toxicology of mercury and its chemical compounds. Crit Rev Toxicol 36(8):609–662, PMID: 16973445, https://doi.org/10.1080/10408440600845619.

Cramer T, Yamanishi Y, Clausen BE, Förster I, Pawlinski R, Mackman N, et al. 2003. HIF-1 alpha is essential for myeloid cell-mediated inflammation. Cell 112(5):645–657, PMID: 12628185, https://doi.org/10.1016/s0092-8674(03)00154-5.

Culbreth M, Aschner M. 2016. Dysregulation of glutamate cycling mediates methylmercury-induced neurotoxicity. Adv Neurobiol 13:295–305, PMID: 27885634, https://doi.org/10.1007/978-3-319-45096-4_11.

Czibik G. 2010. Complex role of the HIF system in cardiovascular biology. J Mol Med 88(11):1101–1111, PMID: 20574807, https://doi.org/10.1007/s00109-010-0646-x.

Das KK, Jargar JG, Saha S, Yendigeri SM, Singh SB. 2015. α-tocopherol supplementation prevents lead acetate and hypoxia-induced hepatic dysfunction. Indian J Pharmacol 47(3):285–291, PMID: 26069366, https://doi.org/10.4103/0253-7613.157126.

Dehne N, Hintereder G, Brüne B. 2010. High glucose concentrations attenuate hypoxia-inducible factor-1α expression and signaling in non-tumor cells. Exp Cell Res 316(7):1179–1189, PMID: 20184881, https://doi.org/10.1016/j.yexcr.2010.02.019.

Deng Y, Xu Z, Xu B, Liu W, Wei Y, Li Y, et al. 2014. Exploring cross-talk between oxidative damage and excitotoxicity and the effects of riluzole in the rat cortex after exposure to methylmercury. Neurotox Res 26(1):40–51, PMID: 24519665, https://doi.org/10.1007/s12640-013-9448-6.

Dong SY, Guo YJ, Feng Y, Cui XX, Kuo SH, Liu T, et al. 2016. The epigenetic regulation of HIF-1α by SIRT1 in MPP(+) treated SH-SY5Y cells. Biochem Biophys Res Commun 470(2):453–459, PMID: 26768367, https://doi.org/10.1016/j.bbrc.2016.01.013.

Fang YT, Guo CJ, Zhang PP, Zhao W, Xing G, Wang S, et al. 2016. Role of autophagy in methylmercury-induced neurotoxicity in rat primary astrocytes. Arch Toxicol 90(2):333–345, PMID: 25488884, https://doi.org/10.1007/s00204-014-1425-1.

Farina M, Aschner M. 2017. Methylmercury-induced neurotoxicity: focus on prooxidative events and related consequences. Adv Neurobiol 18:267–286, PMID: 28889272, https://doi.org/10.1007/978-3-319-60189-2_13.

Farina M, Aschner M, Rocha JB. 2011a. Oxidative stress in MeHg-induced neurotoxicity. Toxicol Appl Pharmacol 256(3):405–417, PMID: 21601588, https://doi.org/10.1016/j.taap.2011.05.001.

Farina M, Rocha JB, Aschner M. 2011b. Mechanisms of methylmercury-induced neurotoxicity: evidence from experimental studies. Life Sci 89(15–16):555–563, PMID: 21683713, https://doi.org/10.1016/j.lfs.2011.05.019.

Feng Y, Liu T, Li XQ, Liu Y, Zhu XY, Jankovic J, et al. 2014. Neuroprotection by Orexin-A via HIF-1α induction in a cellular model of Parkinson's disease. Neurosci Lett 579:35–40, PMID: 25038418, https://doi.org/10.1016/j.neulet.2014.07.014.

Guo C, Hao LJ, Yang ZH, Chai R, Zhang S, Gu Y, et al. 2016. Deferoxamine-mediated up-regulation of HIF-1α prevents dopaminergic neuronal death via the activation of MAPK family proteins in MPTP-treated mice. Exp Neurol 280:13–23, PMID: 26996132, https://doi.org/10.1016/j.expneurol.2016.03.016.

Haase VH. 2017. HIF-prolyl hydroxylases as therapeutic targets in erythropoiesis and iron metabolism. Hemodial Int 21:S110–S124, PMID: 28449418, https://doi.org/10.1111/hdi.12567.

Hamrick SE, McQuillen PS, Jiang X, Mu D, Madan A, Ferriero DM. 2005. A role for hypoxia-inducible factor-1alpha in desferoxamine neuroprotection. Neurosci Lett 379(2):96–100, PMID: 15823423, https://doi.org/10.1016/j.neulet.2004.12.080.

Han J, Lee JS, Choi D, Lee Y, Hong S, Choi J, et al. 2009. Manganese (II) induces chemical hypoxia by inhibiting HIF-prolyl hydroxylase: implication in manganese-induced pulmonary inflammation. Toxicol Appl Pharmacol 235(3):261–267, PMID: 19263519, https://doi.org/10.1016/j.taap.2009.01.003.

Henkel G, Krebs B. 2004. Metallothioneins: zinc, cadmium, mercury, and copper thiolates and selenolates mimicking protein active site features-structural aspects and biological implications. Chem Rev 104(2):801–824, PMID: 14871142, https://doi.org/10.1021/cr020620d.

Hirooka T, Yamamoto C, Yasutake A, Eto K, Kaji T. 2013. Expression of VEGF-related proteins in cultured human brain microvascular endothelial cells and pericytes after exposure to methylmercury. J Toxicol Sci 38(6):837–845, PMID: 24213003, https://doi.org/10.2131/jts.38.837.

Horiguchi H, Kayama F, Oguma E, Willmore WG, Hradecky P, Bunn HF. 2000. Cadmium and platinum suppression of erythropoietin production in cell culture: clinical implications. Blood 96(12):3743–3747, PMID: 11090055, https://doi.org/10.1182/blood.V96.12.3743.h8003743_3743_3747.

Ishihara Y, Tsuji M, Kawamoto T, Yamazaki T. 2016. Involvement of reactive oxygen species derived from mitochondrial in neuronal injury elicited by methylmercury. J Clin Biochem Nutr 59(3):182–190, PMID: 27895385, https://doi.org/10.3164/jcbn.16-19.

Ivan M, Kondo K, Yang H, Kim W, Valiando J, Ohh M, et al. 2001. HIFα targeted for VHL-mediated destruction by proline hydroxylation: implications for O_2 sensing. Science 292(5516):464–468, PMID: 11292862, https://doi.org/10.1126/science.1059817.

Iyalomhe O, Swierczek S, Enwerem N, Chen Y, Adedeji MO, Allard J, et al. 2017. The role of hypoxia-inducible factor 1 in mild cognitive impairment. Cell Mol Neurobiol 37(6):969–977, PMID: 27858285, https://doi.org/10.1007/s10571-016-0440-6.

Jaeckel P, Krauss G, Menge S, Schierhorn A, Rücknagel P, Krauss GJ. 2005. Cadmium induces a novel metallothionein and phytochelatin 2 in an aquatic fungus. Biochem Biophys Res Commun 333(1):150–155, PMID: 15939401, https://doi.org/10.1016/j.bbrc.2005.05.083.

Jain IH, Zazzeron L, Goli R, Alexa K, Schatzman-Bone S, Dhillon H, et al. 2016. Hypoxia as a therapy for mitochondrial disease. Science 352(6281):54–61, PMID: 26917594, https://doi.org/10.1126/science.aad9642.

Jensen CJ, Massie A, De Keyser J. 2013. Immune players in the CNS: the astrocyte. J Neuroimmune Pharmacol 8(4):824–839, PMID: 23821340, https://doi.org/10.1007/s11481-013-9480-6.

Jing Y, Liu LZ, Jiang Y, Zhu Y, Guo NL, Barnett J, et al. 2012. Cadmium increases HIF-1 and VEGF expression through ROS, ERK, and AKT signaling pathways and induces malignant transformation of human bronchial epithelial cells. Toxicol Sci 125(1):10–19, PMID: 21984483, https://doi.org/10.1093/toxsci/kfr256.

Kaur P, Evje L, Aschner M, Syversen T. 2010. The in vitro effects of Trolox on methymercury-induced neurotoxicity. Toxicology 276 (1):73–78, PMID: 20637824, https://doi.org/10.1016/j.tox.2010.07.006.

Koivunen P, Hirsilä M, Remes AM, Hassinen IE, Kivirikko KI, Myllyharju J. 2007. Inhibition of hypoxia-inducible factor (HIF) hydroxylases by citric acid cycle intermediates: possible links between cell metabolism and stabilization of HIF. J Biol Chem 282(7):4524–4532, PMID: 17182618, https://doi.org/10.1074/jbc.M610415200.

LeBel CP, Ali SF, Bondy SC. 1992. Deferoxamine inhibits methyl mercury-induced increases in reactive oxygen species formation in rat brain. Toxicol Appl Pharmacol 112(1):161–165, PMID: 1310167, https://doi.org/10.1016/0041-008X(92)90292-Z.

Lee DW, Rajagopalan S, Siddiq A, Gwiazda R, Yang L, Beal MF, et al. 2009. Inhibition of prolyl hydroxylase protects against 1-methyl-4-phenyl-1,2,3,6-tetrahydropyridine-induced neurotoxicity: model for the potential involvement of the hypoxia-inducible factor pathway in Parkinson disease. J Biol Chem 284(42):29065–29076, PMID: 19679656, https://doi.org/10.1074/jbc.M109.000638.

Lee KA, Roth RA, LaPres JJ. 2007. Hypoxia, drug therapy and toxicity. Pharmacol Ther 113(2):229–246, PMID: 17046066, https://doi.org/10.1016/j.pharmthera.2006.08.001.

Li Q, Chen H, Huang X, Costa M. 2006. Effects of 12 metal ions on iron regulatory protein 1 (IRP-1) and hypoxia-inducible factor-1 alpha (HIF-1α) and HIF-regulated genes. Toxicol Appl Pharmacol 213(3):245–255, PMID: 16386771, https://doi.org/10.1016/j.taap.2005.11.006.

Li X, Cui XX, Chen YJ, Wu TT, Xu H, Yin H, et al. 2018. Therapeutic potential of a prolyl hydroxylase inhibitor FG-4592 for Parkinson's diseases *in vitro* and *in vivo*: regulation of redox biology and mitochondrial function. Front Aging Neurosci 10:121, PMID: 29755339, https://doi.org/10.3389/fnagi.2018.00121.

Liao TL, Chen SC, Tzeng CR, Kao SH. 2014. TCDD induces the hypoxia-inducible factor (HIF)-1α regulatory pathway in human trophoblastic JAR cells. Int J Mol Sci 15(10):17733–17750, PMID: 25272228, https://doi.org/10.3390/ijms151017733.

Liu W, Shen SM, Zhao XY, Chen GQ. 2012. Targeted genes and interacting proteins of hypoxia inducible factor-1. Int J Biochem Mo Biol 3(2):165–178, PMID: 22773957.

Liu W, Xu Z, Deng Y, Xu B, Wei Y, Yang T. 2013. Protective effects of memantine against methylmercury-induced glutamate dyshomeostasis and oxidative stress in rat cerebral cortex. Neurotox Res 24(3):320–337, PMID: 23504438, https://doi.org/10.1007/s12640-013-9386-3.

Liu W, Xu Z, Deng Y, Xu B, Yang H, Wei Y, et al. 2014. Excitotoxicity and oxidative damages induced by methylmercury in rat cerebral cortex and the protective effects of tea polyphenols. Environ Toxicol 29(3):269–283, PMID: 22223486, https://doi.org/10.1002/tox.21755.

Mailloux RJ, Appanna VD. 2007. Aluminum toxicity triggers the nuclear translocation of HIF-1α and promotes anaerobiosis in hepatocytes. Toxicol In Vitro 21(1):16–24, PMID: 16979867, https://doi.org/10.1016/j.tiv.2006.07.013.

Mailloux RJ, Puiseux-Dao S, Appanna VD. 2009. Alpha-ketoglutarate abrogates the nuclear localization of HIF-1α in aluminum-exposed hepatocytes. Biochimie 91(3):408–415, PMID: 19028544, https://doi.org/10.1016/j.biochi.2008.10.014.

Marxsen JH, Stengel P, Doege K, Heikkinen P, Jokilehto T, Wagner T, et al. 2004. Hypoxia-inducible factor-1 (HIF-1) promotes its degradation by induction of HIF-alpha-prolyl-4-hydroxylases. Biochem J 381(Pt 3):761–767, PMID: 15104534, https://doi.org/10.1042/BJ20040620.

Matsumoto K, Imagawa S, Obara N, Suzuki N, Takahashi S, Nagasawa T, et al. 2006. 2-Oxoglutarate downregulates expression of vascular endothelial growth factor and erythropoietin through decreasing hypoxia-inducible factor-1alpha and inhibits angiogenesis. J Cell Physiol 209(2):333–340, PMID: 16883594, https://doi.org/10.1002/jcp.20733.

Mense SM, Sengupta A, Zhou M, Lan C, Bentsman G, Volsky DJ, et al. 2006. Gene expression profiling reveals the profound upregulation of hypoxia-responsive genes in primary human astrocytes. Physiol Genomics 25(3):435–449, PMID: 16507782, https://doi.org/10.1152/physiolgenomics.00315.2005.

Pan R, Chen C, Liu WL, Liu KJ. 2013. Zinc promotes the death of hypoxic astrocytes by upregulating hypoxia-induced hypoxia-inducible factor-1alpha expression via poly (ADP-ribose) polymerase-1. CNS Neurosci Ther 19(7):511–520, PMID: 23582235, https://doi.org/10.1111/cns.12098.

Pan Y, Mansfield KD, Bertozzi CC, Rudenko V, Chan DA, Giaccia AJ, et al. 2007. Multiple factors affecting cellular redox status and energy metabolism modulate hypoxia-inducible factor prolyl hydroxylase activity in vivo and in vitro. Mol Cell Biol 27(3):912–925, PMID: 17101781, https://doi.org/10.1128/MCB.01223-06.

Parada-Bustamante A, Valencia C, Reuquen P, Diaz P, Rincion-Rodriguez R, Orihuela PA. 2015. Role of 2-methoxyestradiol, an endogenous estrogen metabolite, in health and disease. Mini Rev Med Chem 15(5):427–438, PMID: 25723461, https://doi.org/10.2174/1389557515666150226121052.

Park YH, Bae HC, Kim J, Jeong SH, Yang SI, Son SW. 2018. Zinc oxide nanoparticles induce HIF-1α protein stabilization through increased reactive oxygen species generation from electron transfer chain complex III of mitochondria. J Dermatol Sci 91(1):104–107, PMID: 29622477, https://doi.org/10.1016/j.jdermsci.2018.03.010.

Polunas M, Halladay A, Tjalkens RB, Philbert MA, Lowndes H, Reuhl K. 2011. Role of oxidative stress and the mitochondrial permeability transition in methylmercury cytotoxicity. Neurotoxicology 32(5):526–534, PMID: 21871920, https://doi.org/10.1016/j.neuro.2011.07.006.

Pribluda VS, Gubish ER Jr, Lavallee TM, Treston A, Swartz GM, Green SJ. 2000. 2-Methoxyestradiol: an endogenous antiangiogenic and antiproliferative drug candidate. Cancer Metastasis Rev 19(1–2):173–179, PMID: 11191057, https://doi.org/10.1023/a:1026543018478.

Rothenberg SE, Windham-Myers L, Creswell JE. 2014. Rice methylmercury exposure and mitigation: A comprehensive review. Environ Res 133:407–423, PMID: 24972509, https://doi.org/10.1016/j.envres.2014.03.001.

Rudge JS, Li Y, Pasnikowski EM, Mattsson K, Pan L, Yancopoulos GD, et al. 1994. Neurotrophic factor receptors and their signal transduction capabilities in rat astrocytes. Eur J Neurosci 6(5):693–705, PMID: 8075814, https://doi.org/10.1111/j.1460-9568.1994.tb00981.x.

Santos AAD, Hort MA, Culbreth M, López-Granero C, Farina M, Rocha JB, et al. 2016. Methylmercury and brain development: a review of recent literature. J Trace Elem Med Biol 38:99–107, PMID: 26987277, https://doi.org/10.1016/j.jtemb.2016.03.001.

Santos AAD, López-Granero C, Farina M, Rocha JB, Bowman AB, Aschner M. 2018. Oxidative stress, caspase-3 activation and cleavage of ROCK-1 play an essential role in MeHg-induced cell death in primary astroglial cells. Food Chem Toxicol 113:328–336, PMID: 29428217, https://doi.org/10.1016/j.fct.2018.01.057.

Sato M, Kondoh M. 2002. Recent studies on metallothionein: protection against toxicity of heavy metals and oxygen free radicals. Tohoku J Exp Med 196(1):9–22, PMID: 12498322, https://doi.org/10.1620/tjem.196.9.

Semenza G. 2002. Signal transduction to hypoxia-inducible factor 1. Biochem Pharmacol 64(5–6):993–998, PMID: 12213597, https://doi.org/10.1016/S0006-2952(02)01168-1.

Semenza GL, Wang GL. 1992. A nuclear factor induced by hypoxia via de novo protein synthesis binds to the human erythropoietin gene enhancer at a site required for transcriptional activation. Mol Cell Biol 12(12):5447–5454, PMID: 1448077, https://doi.org/10.1128/mcb.12.12.5447.

Sen T, Sen N. 2016. Treatment with an activator of hypoxia-inducible factor 1, DMOG provides neuroprotection after traumatic brain injury. Neuropharmacology 107:79–88, PMID: 26970014, https://doi.org/10.1016/j.neuropharm.2016.03.009.

Shanker G, Syversen T, Aschner M. 2003. Astrocyte-mediated methylmercury neurotoxicity. BTER 95(1):1–10, PMID: 14555794, https://doi.org/10.1385/BTER:95:1:1.

Shapiro AM, Chan HM. 2008. Characterization of demethylation of methylmercury in cultured astrocytes. Chemosphere 74(1):112–118, PMID: 18950830, https://doi.org/10.1016/j.chemosphere.2008.09.019.

Shin HJ, Choi MS, Ryoo NH, Nam KY, Park GY, Bae JH, et al. 2010. Manganese-mediated up-regulation of HIF-1alpha protein in Hep2 human laryngeal epithelial cells via activation of the family of MAPKs. Toxicol In Vitro 24(4):1208–1214, PMID: 20152896, https://doi.org/10.1016/j.tiv.2010.02.008.

Siddiq A, Ayoub IA, Chavez JC, Aminova L, Shah S, LaManna JC, et al. 2005. Hypoxia-inducible factor prolyl 4-hydroxylase inhibition. A target for neuroprotection in the central nervous system. J Biol Chem 280(50):41732–41743, PMID: 16227210, https://doi.org/10.1074/jbc.M504963200.

Soucek T, Cumming R, Dargusch R, Maher P, Schubert D. 2003. The regulation of glucose metabolism by HIF-1 mediates a neuroprotective response to amyloid beta peptide. Neuron 39(1):43–56, PMID: 12848931, https://doi.org/10.1016/S0896-6273(03)00367-2.

Steuerwald U, Weihe P, Jørgensen PJ, Bjerve K, Brock J, Heinzow B, et al. 2000. Maternal seafood diet, methylmercury exposure and neonatal neurologic function. J Pediatr 136(5):599–605, PMID: 10802490, https://doi.org/10.1067/mpd.2000.102774.

Stopford W, Goldwater LJ. 1975. Methylmercury in the environment: a review of current understanding. Environ Health Perspect 12:115–118, PMID: 1227851, https://doi.org/10.1289/ehp.7512115.

Sun Y, Li QF, Zhang Y, Hu R, Jiang H. 2013. Isoflurane preconditioning increases survival of rat skin random-pattern flaps by induction of HIF-1α expression. Cell Physiol Biochem 31(4–5):579–591, PMID: 23635649, https://doi.org/10.1159/000350078.

Triantafyllou A, Liakos P, Tsakalof A, Georgatsou E, Simos G, Bonanou S. 2006. Cobalt induces hypoxia-inducible factor-1alpha (HIF-1alpha) in HeLa cells by an iron-independent, but ROS-, PI-3K and MAPK-dependent mechanism. Free Radic Res 40(8):847–856, PMID: 17015263, https://doi.org/10.1080/10715760600730810.

Wikenheiser J, Karunamuni G, Sloter E, Walker MK, Roy D, Wilson DL, et al. 2013. Altering HIF-1α through 2,3,7,8-tetrachlorodibenzo-p-dioxin (TCDD) exposure affects coronary vessel development. Cardiovasc Toxicol 13(2):161–167, PMID: 23264063, https://doi.org/10.1007/s12012-012-9194-7.

Wu Y, Li X, Xie W, Jankovic J, Le W, Pan T. 2010. Neuroprotection of deferoxamine on rotenone-induced injury via accumulation of HIF-1 alpha and induction of autophagy in SH-SY5Y cells. Neurochem Int 57(3):198–205, PMID: 20546814, https://doi.org/10.1016/j.neuint.2010.05.008.

Yang B, Bai Y, Yin C, Qian H, Xing G, Wang S, et al. 2018. Activation of autophagic flux and the Nrf2/ARE signaling pathway by hydrogen sulfide protects against acrylonitrile-induced neurotoxicity in primary rat astrocytes. Arch Toxicol 92(6):2093–2108, PMID: 29725710, https://doi.org/10.1007/s00204-018-2208-x.

Yee S, Choi BH. 1996. Oxidative stress in neurotoxic effects of methylmercury poisoning. Neurotoxicology 17(1):17–26, PMID: 8784815.

Yin Z, Lee E, Ni M, Jiang H, Milatovic D, Rongzhu L, et al. 2011. Methylmercury-induced alterations in astrocyte functions are attenuated by ebselen. Neurotoxicology 32(3):291–299, PMID: 21300091, https://doi.org/10.1016/j.neuro.2011.01.004.

Zhang H, Feng XB, Larssen T, Qiu GL, Vogt RD. 2010. In inland China, rice, rather than fish, is the major pathway for methylmercury exposure. Environ Health Perspect 118(9):1183–1188, PMID: 20378486, https://doi.org/10.1289/ehp.1001915.